Journal of Magnetic Resonance 199 (2009) 159–165

Contents lists available at ScienceDirect

Journal of Magnetic Resonance

journal homepage: www.elsevier.com/locate/jmr

Sequentially acquired two-dimensional NMR spectra from hyperpolarized sample

Haifeng Zeng, Sean Bowen, Christian Hilty *

Texas A&M University, Chemistry Department, 3255 TAMU, College Station, TX 77843, USA

ARTICLE INFO

Article history:
Received 30 January 2009
Revised 7 April 2009
Available online 24 April 2009

Keywords:
Nuclear magnetic resonance
Dynamic nuclear polarization
Correlation spectroscopy

ABSTRACT

A scheme capable of acquiring heteronuclear 2D NMR spectra of hyperpolarized sample is described. Hyperpolarization, the preparation of nuclear spins in a polarized state far from thermal equilibrium, can increase the NMR signal by several orders of magnitude. It presents opportunities to apply NMR spectroscopy to dilute samples that would otherwise yield insufficient signal. However, conventional 2D NMR spectroscopy, which is commonly applied for the determination of molecular structure, relies on the recovery of the initial polarization after each transient. For this reason, it cannot be applied directly to a sample that has been hyperpolarized once. With appropriately modified pulse schemes, two-dimensional NMR spectra an however be acquired sequentially by utilizing a small portion of the hyperpolarized signal in every scan, while keeping the remaining polarization for future scans. We present heteronuclear multi-quantum spectra of single hyperpolarized samples using this technique, and discuss different options for distributing the polarization among different scans. This robust method takes full advantage of Fourier NMR to resolve overlapping chemical shifts, and may prove particularly useful for the structural elucidation of compounds in mass-limited samples.

1. Introduction

Ex-situ dynamic nuclear polarization (DNP) [1,2] is an emerging technology that allows the acquisition of liquid-state NMR spectra with greatly enhanced sensitivity [3–6]. Using this technique, a sample aliquot is polarized in the solid state at low temperature, where the DNP process is the most efficient. The sample is subsequently dissolved in a stream of hot solvent, while maintaining polarization, and rapidly injected into an NMR spectrometer for acquisition of an NMR spectrum.

One of the potential drawbacks of using ex-situ DNP is that, once the polarization has been converted into an observable coherence, the spin system returns to the non-polarized state given by the Boltzmann population. While DNP makes available a high NMR signal level, the polarization provided by this technique can be used only once. In the most straight-forward application of ex-situ DNP, a single one-dimensional spectrum is acquired with high sensitivity. One-dimensional spectra however carry only a limited amount of information, and in many applications, including structural elucidation of organic molecules, two-dimensional NMR spectroscopy has long been a standard technique. Conventional 2D NMR experiments, where the spin system reaches an equilibrium state between successive scans, cannot be applied to such polarized samples. However, for these applications to benefit from the signal enhancement provided by DNP-NMR, it is necessary to find ways of making two-dimensional NMR spectroscopic techniques amenable to DNP polarized samples. Several strategies have been proposed towards this end. Firstly, in single-scan 2D NMR, pulsed field gradients are utilized to selectively address spatial regions; all of the "scans" necessary for a two-dimensional spectrum are acquired simultaneously from different regions of the sample [4,7]. Secondly, in our own previous work, we proposed a scheme to derive two-dimensional chemical shift correlations using differential scaling of the observed scalar coupling by off-resonance decoupling, without explicitly acquiring a two-dimensional NMR spectrum [8]. As a third option, it is possible to acquire two-dimensional NMR spectra in sequential scans from one single hyperpolarized sample, using variable flip angles [9,10]. The technique employing off-resonance decoupling is particularly robust and easy to implement, however for larger molecules does not permit the resolution of overlapped resonances. The other two techniques both allow the acquisition of a true two-dimensional dataset. On one hand, single scan NMR is an elegant way of achieving this goal, and its application to hyperpolarized sample has been investigated [4,10]. On the other hand, the simplicity of sequential acquisition of two-dimensional NMR spectra rivals that of the pseudo one-dimensional, off-resonance decoupling scheme. Additionally it gains the major advantage of two-dimensional NMR spectroscopy, its ability to resolve overlapped chemical shifts through dispersion in the second dimension. Although it is slower than single-scan 2D NMR, it is significantly easier to implement, and is particularly robust against residual fluid motion in the sample caused by rapid injection of DNP polarized sample. For these

* Corresponding author. Fax: +1 979 862 4237.
E-mail address: chilty@mail.chem.tamu.edu (C. Hilty).

1090-7807/$ - see front matter © 2009 Elsevier Inc. All rights reserved.
doi:10.1016/j.jmr.2009.04.011

reasons, its application to hyperpolarized sample in the context of structural elucidation of organic compounds merits investigation. Here, we compare heteronuclear correlation spectra [11,12] of hyperpolarized samples, using different strategies for sequential acquisition of the indirect chemical shift dimension. In addition, the effects of two different flip angle series for excitation are tested, and the consequences of the respective methods are discussed.

2. Experimental

2.1. Sample preparation

(1) Sample for measurement of [^{13}C,^{1}H]-HMQC spectrum: 0.5 μL 3.6 M vanillin in a solution of 72% DMSO-d6 and 28% D_2O (Cambridge Isotope Laboratories, Andover, MA) with 15 mM 4-Hydroxy-2,2,6,6-tetramethylpiperidine-1-oxyl (TEMPOL) free radical (Sigma–Aldrich, St. Louis, MO). (2) Sample for testing the effect of variable flip angle series: 0.2 μL 3.6 M vanillin in a solution of 72% DMSO-d6 and 28% D_2O with 15 mM 4-Hydroxy-2,2,6,6-tetramethylpiperidine-1-oxyl (TEMPOL) free radical. (3) Sample for [^{1}H,^{13}C]-HMQC spectrum: 2.0 μL 3.6 M vanillin in a solution of 72% DMSO-d6 and 28% D_2O with 15 mM tris[8-carboxyl-2,2,6,6-tetramethyl-benzo(1,2-d:4,5-d′)bis(1,3)dithiole-4-yl]methyl sodium salt free radical (“Finland”; Oxford Instruments, Tubney Woods, UK).

2.2. DNP polarization

DNP polarization took place in an Oxford Instruments HyperSense DNP polarizer at a temperature of 1.3 K. For [^{13}C,^{1}H]-HMQC experiments and variable flip angle series test, 100 mW of microwave power was applied at a frequency of 94.270 GHz for a duration of 30 min. In [^{1}H,^{13}C]-HMQC experiments, the microwave power was 60 mW, the frequency 93.977 GHz and the polarization time 5.5 h. After polarization, samples were dissolved into acetonitrile, except for the flip angle test experiments shown in Fig. 5, where acetonitrile-d3 was used. For dissolution, 4 mL of solvent was heated until a pressure of 10 bar was achieved, flushed over the frozen sample, and injected into the NMR spectrometer using a homebuilt sample injector [13]. NMR spectra were acquired ca. 2.5 s after the start of dissolution. Post-dissolution sample concentrations were determined by HPLC following the NMR experiment. Typical final sample concentrations were in the low mM range (see below).

2.3. NMR spectroscopy

Acquisition of the NMR spectrum was automatically triggered by a signal from the sample injector. Pulse sequences for [^{13}C,^{1}H]-HMQC and [^{1}H,^{13}C]-HMQC experiments are shown in Fig. 1. Raw NMR data was processed using the program TOPSPIN by Bruker. Fourier transformation was performed along the t_2 and t_1 dimension in the same way that a conventional NMR spectrum would be processed. Spectra obtained using [^{13}C,^{1}H]-HMQC pulse sequences without ^{1}H π pulses contain a ^{1}H chemical shift dependence in the ^{13}C dimension. These spectra were processed using the MATLAB program, where this chemical shift dependence could be removed by multiplication with an offset dependent phase factor prior to Fourier transformation (see below).

3. Results and discussion

Fast heteronuclear multi-quantum correlation experiments, [^{13}C,^{1}H]-HMQC and [^{1}H,^{13}C]-HMQC, were measured with the pulse sequences illustrated in Fig. 1, using DNP-polarized samples of vanillin. The indirect dimension was obtained from a Fourier transform of transients that were sequentially acquired from a single hyperpolarized sample, with a total experimental duration of 1.4–3 s. Heteronuclear multi quantum coherence (HMQC) transfer ideally lends itself to the implementation of a multi transient experiment from hyperpolarized sample, because the small number of required pulses in a given scan allows the conservation of the remaining unused longitudinal magnetization for the subsequent scans. For excitation, a variable flip angle [9] was used to convert the same amount of longitudinal magnetization (polarization) into observable coherence in each scan.

3.1. [^{13}C,^{1}H]-HMQC experiment

The pulse sequence in Fig. 1a represents the adaptation of an HMQC experiment [11,18] for use with sample hyperpolarized on its ^{1}H nuclei. This sequence contains only two pulses on the radio frequency channel corresponding to the polarized nuclei: the small

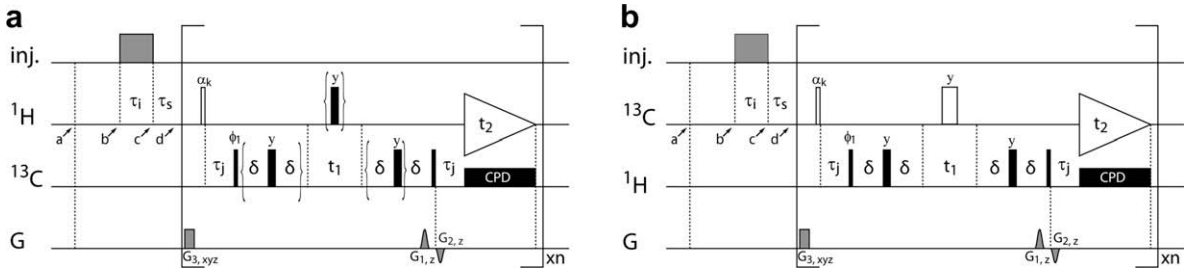

Fig. 1. Pulse sequences for measurement of a 2D NMR spectrum of hyperpolarized sample, using (a) [^{13}C,^{1}H]-HMQC and (b) [^{1}H,^{13}C]-HMQC. An Oxford Instruments HyperSense DNP polarizer and a Bruker 400 MHz NMR spectrometer were used. Sample was delivered from the DNP polarizer to a home built sample injector between time points a and b. Sample injection into the NMR took place during τ_i = 325 ms, and the NMR experiment was triggered after a stabilization time τ_s = 200 ms at time point d. The two-dimensional dataset consists of n = 32 transients, recorded by incrementing the evolution time t_1 and phase φ_1, using the States-TPPI method [14,15]. $G_{3,xyz}$ = (25..50;25..50;25..50 G/cm, 0.4 ms) removes unwanted coherence prior to the next acquisition. Its value was adjusted randomly within the indicated range, for each scan. The flip angles α_k of the excitation pulse (pulse strength γB_1 = 25 kHz) are adjusted to provide the same fraction of magnetization in each transient (see text). Narrow and wide black bars represent 90° and 180° pulses, and the phases are x unless indicated otherwise. Coherence selection is achieved by the pulsed field gradients $G_{1,z}$ and $G_{2,z}$. (a) [^{13}C,^{1}H]-HMQC spectra, $G_{1,z}$ = 50 G/cm and $G_{2,z}$ = −37.4 G/cm for zero-quantum version, $G_{1,z}$ = −40 G/cm and $G_{2,z}$ = 50 G/cm for double quantum version. The gradient time is 1 ms, and δ = 1.2 ms. $\tau_j = 1/(2J_{CH})$ = 3.12 ms. The delays and pulses in the brackets are deleted in the version without refocusing. During each acquisition period, 32,768 points are acquired, using $t_{2,max}$ = 33 ms. ^{13}C composite pulse decoupling (CPD) is applied using GARP [16] at a field strength γB_1 = 2.38 kHz. The carrier is set to 140 ppm on ^{13}C and 7 ppm on ^{1}H. The spectral width of ^{13}C is 250 ppm. (b) [^{1}H,^{13}C]-HMQC spectra, $G_{1,z}$ and $G_{2,z}$ are 16.8 and 50 G/cm, respectively. The gradient time is 500 μs, and δ = 700 μs. $\tau_j = 0.3/J_{CH}$ = 1.88 ms. During each acquisition period, 16,384 points are acquired, and $t_{2,max}$ = 82 ms. ^{1}H CPD is applied at a field strength γB_1 = 2.31 kHz. The carrier is set to 6.0 ppm on ^{1}H and 100 ppm on ^{13}C. The spectral width of ^{1}H is 12.0 ppm. The wide open bar on ^{13}C stands for a composite π pulse, which is (3π/2 − y, 2πy, π/2 − x, 3π/2x, 2π − x, π/2y) [17].

flip angle pulse for excitation, and the π pulse for refocusing of chemical shift [18]. The resulting data can be processed using present-day NMR software without the need for additional scripts, and the resulting spectra can be presented in phase sensitive mode. The π pulse on the ^{1}H channel pulse does not alter the amount of the remaining polarization (i.e. longitudinal magnetization) after each transient, as it merely transforms the product operators I_z into $-I_z$. A spectrum acquired using this scheme is shown in Fig. 2. This experiment is most closely related to a conventional heteronuclear correlation experiment. Most importantly, it allows the resolution of chemical shifts that would otherwise be overlapped, or nearly overlapped, in a one-dimensional experiment (such as peaks B and D in Fig. 2). The number of points acquired in the ^{1}H dimension was 32,768, and in the ^{13}C dimension was 32. The large number of points in the ^{1}H dimension was selected to reduce the sampling interval, enabling the use of a digital filter in the relatively short duration (33 ms) of each of the free induction decays [19]. The data presented in Fig. 2 were acquired using a total acquisition time of 1.55 s of a sample at a concentration of 0.91 mM, corresponding to a concentration of 9.7 μM of the NMR active ^{13}C isotope.

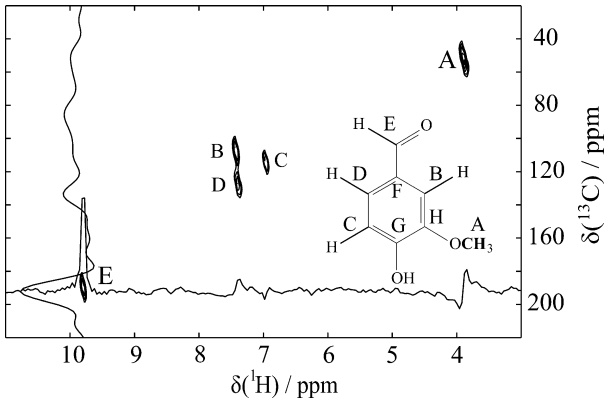

Fig. 2. [^{13}C,^{1}H]-HMQC spectrum of vanillin with a total acquisition time of 1.55 s. The experiment shown in Fig. 1a was used, including the elements in the brackets. The acquisition parameters are in the caption of the pulse sequence. The data were zero filled to 128 × 32,768 points, and processed with a 20 Hz line broadening exponential window function in the F2 dimension and Fourier transformed in both dimensions.

A spectrum acquired by this method may suffer from artifacts if the refocusing pulse is imperfect due to B_1 inhomogeneity, slight miscalibration of the pulse length, or off-resonance effects. These imperfections can influence the remaining polarization after each scan in a cumulative manner. Their effect is observable as small distortions of the baseline in the traces plotted through the spectrum in Fig. 2. An alternative option for recording this spectrum is by removing the refocusing π pulse on ^{1}H, leaving only the single variable flip angle pulse used for excitation of the coherence on this channel. Fig. 3a and c show spectra acquired using a simplified scheme, where the bracketed pulse sequence elements in Fig. 1a have been removed. The experiment can be implemented either with double-quantum (DQ; Fig. 3a), or with zero-quantum coherence selection (ZQ; Fig. 3c). Due to the absence of a refocusing pulse, however, the chemical shifts of proton and carbon nuclei evolve concurrently during the evolution time t_1. The resulting indirect spectral dimension corresponds to the sum or the difference of the two chemical shifts depending on the gradient selection of double quantum coherence or zero quantum coherence, respectively. Without loss of general applicability, however, the proton chemical shift dependence can be removed by applying an offset dependent shift to the dataset. In (a), zero-quantum

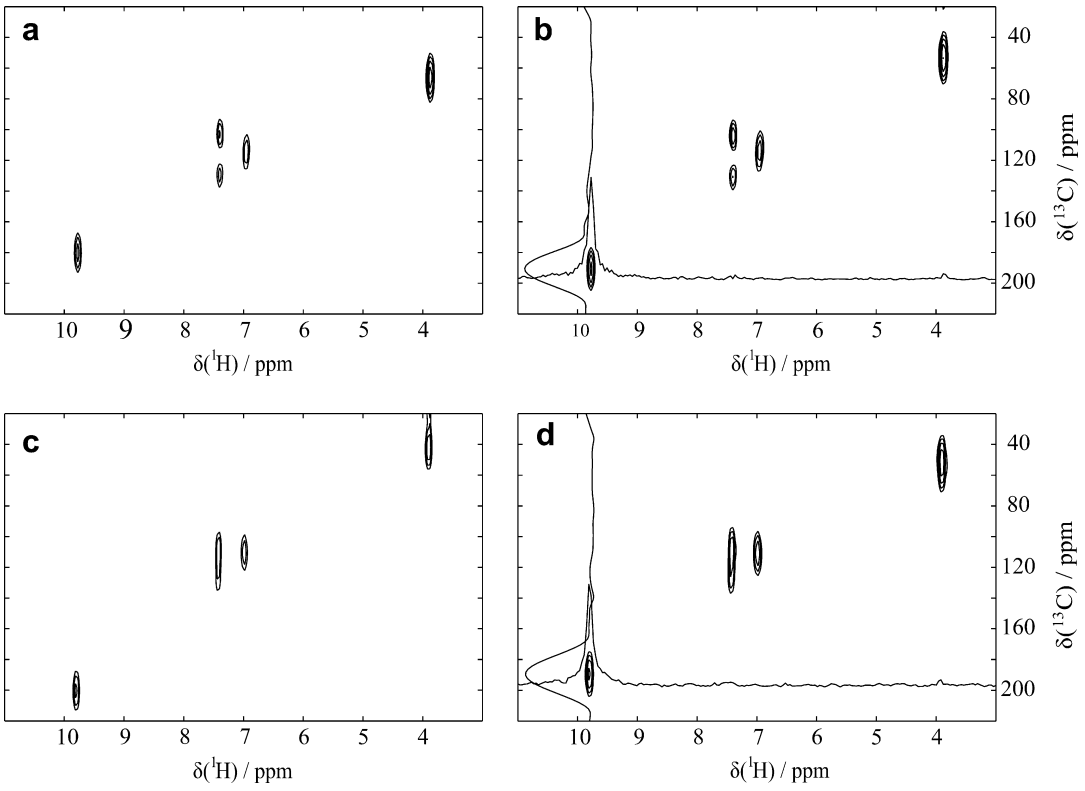

Fig. 3. (a) Original Zero quantum (ZQ) coherence selection HMQC spectrum of vanillin. (b) Permutated ZQ HMQC spectrum. (c) Original Double quantum (DQ) coherence selection HMQC spectrum of vanillin. (d) Permutated DQ HMQC spectrum. The spectra were acquired using the pulse sequence shown in Fig. 1a, with the elements in brackets removed. The acquisition parameters are given in the caption of the pulse sequence. The total acquisition time was 1.44 s. The data was zero filled to 128 × 32,768 points, and processed with an exponential window function using 20 Hz line broadening in the F2 dimension.

coherence selection requires a cyclic permutation $\omega_C \rightarrow \omega_C + (\omega_H - \omega_H^0)$ in the spectrum, which can be achieved most conveniently by multiplying each column of the dataset with the offset dependent factor $e^{i(w_H - w_H^0)}$ prior to Fourier transformation of the indirect dimension. In (c) double quantum coherence selection requires the cyclic permutation $\omega_C \rightarrow \omega_C - (\omega_H - \omega_H^0)$ in the spectrum, which is achieved by multiplication with $e^{-i(w_H - w_H^0)}$ prior to Fourier transformation of the indirect dimension. Resulting from this operation are spectra with identical chemical shifts, shown in panels b and d of Fig. 3. In contrast to the spectra in Fig. 2, the spectra in Fig. 3 need to be presented in absolute value mode. This contributes to a slight broadening of the resonances, which may however be negligible compared to the achievable spectral resolution. The stated disadvantages should be weighed against the cleaner appearance of the baseline in these spectra, as evident from the traces in Fig. 3. For this reason, the modified experiment depicted in Fig. 3 may well be superior for the routine acquisition of heteronuclear 2D spectra of hyperpolarized sample.

3.2. [^{1}H,^{13}C]-HMQC experiment

The experiments presented in Figs. 2 and 3 make use of detection of hyperpolarized ^{1}H nuclei, and most closely resemble conventional [^{13}C,^{1}H]-HMQC experiments. In our experience, typical signal enhancements for hyperpolarized carbon spins (~10,000×) are however higher than typical enhancements for protons (~1000×). Certainly, part of this disadvantage is compensated for by the higher gyromagnetic ratio of protons, which increases the detection sensitivity by $(\gamma_{^1H}/\gamma_{^{13}C})^{3/2} = 7.93$ [20]. Nevertheless, it may be interesting to consider the reverse [^{1}H,^{13}C]-HMQC experiment, where hyperpolarization as well as NMR signal acquisition is carried out on ^{13}C nuclei. The pulse sequence for this experiment is shown in Fig. 1b, and the resulting spectrum is presented in Fig. 4. Apart from an exchange of the two radio-frequency channels, it should be noted that in this case, the application of a refocusing pulse during the indirect chemical shift evolution is compulsory. In the absence of such a pulse, as a consequence of the large chemical shift range of ^{13}C, the indirectly detected sum or difference of chemical shifts, $\omega_H + (\omega_C - \omega_C^0)$ or $\omega_H - (\omega_C - \omega_C^0)$, would significantly exceed the ^{1}H spectral width. Increasing the spectral width of the indirect dimension to cover this broad range would have a detrimental effect on the spectral resolution that is achievable with a given number of scans. Even though the pure ω_H spectrum could still be reconstructed by the same cyclic permutation as described above, it is possible that, prior to permutation, some signal peaks would be shifted to the very edge of the spectrum, where noise is most significant. Again, because of the large chemical shift range of ^{13}C, we use a composite π pulse to minimize the off-resonance effects [17]. Finally, the [^{1}H,^{13}C]-HMQC experiment differs from the [^{13}C,^{1}H]-HMQC experiment in that the possibility exists for having $n = 1..3$ ^{1}H atoms attached to an originally excited ^{13}C atom. Each case would require a different time delay τ for optimum coherence transfer. A good compromise is, however, $\tau = 0.25/J_{CH}$ to $0.3/J_{CH}$. Since in all of these experiments, the spectral resolution in the indirect dimension is limited by the number of points that can be acquired (here, 32 points were used with an acquisition time of 82 ms per point), the choice of using the [^{1}H,^{13}C]-HMQC experiment in Fig. 4 over the [^{13}C,^{1}H]-HMQC experiment in Figs. 2 and 3 will largely depend on whether higher resolution is desired in the ^{1}H or the ^{13}C dimension.

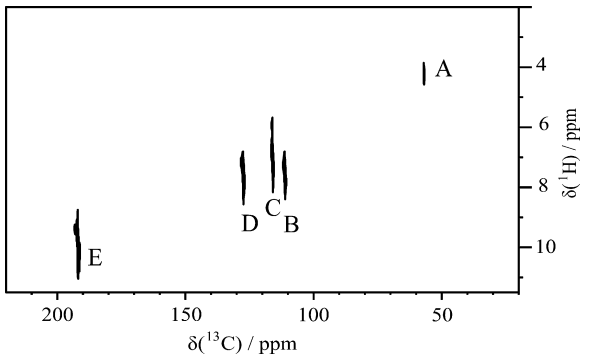

Fig. 4. [^{1}H,^{13}C]-HMQC spectrum of vanillin with a total acquisition time 3.03 s, measured using the pulse sequence in Fig. 1b. The acquisition parameters are in the caption of the pulse sequence. The data was zero filled to 128 × 32,768 points, and processed with an exponential window function using 20 Hz line broadening in the F2 dimension and a cosine window function in the F1 dimension. The letters correspond to those given in the drawing of vanillin in Fig. 2.

3.3. Variable flip angle

The experiments presented above make use of a variable flip angle so that every scan converts the same amount of polarization into observable coherence. In the absence of relaxation, the variable flip angle of the kth scan is given by [8,9,13]

$$\alpha_k = \arcsin\sqrt{\frac{1}{n+1-k}} \tag{1}$$

where n is total number of scans and $k = 1..n$. It should be noted that according to Eq. (1), the flip angle for the last scan is always π/2, so that the last scan can make use of all of the remaining magnetization. The assumption that relaxation is insignificant is true when the experiment time is significantly shorter than the spin-lattice relaxation time (T_1). If this is not the case, later scans will give rise to less signal than earlier scans, and relaxation must be considered in the calculation of the flip angles [9]. A closed form of an equation for flip angles that compensate for relaxation effects can be derived as follows. Let α_k be the flip angle used for acquiring the kth scan, and s_k be the polarization prior to the kth scan. We require that each scan generates the same signal, and that the last scan utilizes all of the remaining polarization through the use of a π/2 pulse, so that

$$s_n = s_k \sin(\alpha_k) \tag{2}$$

Taking relaxation into account,

$$s_{k+1} = \beta s_k \cos(\alpha_k), \tag{3}$$

Where $\beta = e^{-t/T_1}$, t is the time between scans and T_1 is the relaxation time.

Eliminating α_k by combining Eqs. (2) and (3),

$$s_n^2 + \frac{s_{k+1}^2}{\beta^2} = s_k^2 \tag{4}$$

Eq. (4) can be expanded into

$$s_{k+1}^2 + \frac{\beta^2 s_n^2}{1-\beta^2} = \beta^2\left(s_k^2 + \frac{\beta^2 s_n^2}{1-\beta^2}\right). \tag{5}$$

Defining

$$f_k = s_k^2 + \frac{\beta^2 s_n^2}{1-\beta^2} \tag{6}$$

yields

$$f_{k+1} = \beta^2 f_k \tag{7}$$

This is a geometric sequence, and

$$f_k = \beta^{2(k-n)} f_n \tag{8}$$

Using

$$f_n = \frac{s_n^2}{1-\beta^2} \text{ together with Eqs. 2 and 8,} \tag{9}$$

$$\alpha_k = \arcsin\sqrt{\frac{1-\beta^2}{\beta^{2(k-n)}-\beta^2}}, \tag{10}$$

which defines the flip angle series that takes relaxation into consideration. It should be noted that Eq. (10) reduces to Eq. (1) in the limit of $T_1 \to \infty$.

The difference between these two flip angle series in a case where relaxation cannot be neglected can be seen in the experimental data shown in Fig. 5. In Fig. 5a, peak integrals from a series of 1D ^{1}H spectra acquired of a hyperpolarized vanillin sample using the flip angles of Eq. (1) are plotted. The delay between scans was chosen to be 200 ms, yielding a total experimental time of 6.4 s. This time is large compared to the relaxation time of vanillin (2.5 s for proton A, and from 5.0 to 5.7 s for protons B–E). Consequently, there is a sharp decrease in signal intensity for all nuclei. On the other hand, the flip angles used to obtain the data shown in Fig. 5b were calculated using Eq. (4), assuming a value of 5 s for the relaxation time T_1. It can be seen that in this case, the signals for protons B–E, which have matching relaxation times, remain virtually constant. The signal of proton A decays, albeit at a lower rate, because the relaxation time of this proton is shorter than the relaxation time used to calculate the flip angles.

We attribute the slight increase in signal in the last scan to the cumulative effect of imperfections in the preceding small-flip angle excitation pulses or sample movement, leaving slightly more than the calculated amount of polarization for the final $\pi/2$ excitation pulse. Furthermore, variations of signal intensities throughout the experiment due to cross-relaxation are possible.

It should be noted that because of the relatively long relaxation times of spins in the vanillin molecule, to accentuate the relaxation effect the delay time between scans for the data in Fig. 5 (200 ms) is larger than the delay time that was used for acquisition of the spectra in Figs. 2–4 (45–95 ms). Under the conditions used for the 2D spectra, relaxation was negligible for the vanillin molecule, and consequently, Eq. (1) was used for calculating the flip angle.

With flip angles calculated by Eq. (1), the reduction in signal intensity with increasing scan number is more pronounced if a longer experiment time is used (see Fig. 5a), or if the spin-lattice relaxation time is shorter. In these cases, the effect on the spectra is a broadening of peaks in the indirect dimension similar to the application of a window function $e^{-(k-1)t/T_1}$ prior to Fourier transformation [21]. It may then be advantageous to use flip angles calculated by Eq. (10) to obtain a narrower line shape. If flip angles are calculated using an assumed relaxation time $T_{1,assumed}$, which may be different from the actual relaxation time $T_{1,actual}$, the envelope of the signal in the indirect dimension is

$$I_{rel}(k) = e^{-\frac{(k-1)t}{T_{1,actual}}+\frac{(k-1)t}{T_{1,assumed}}}. \tag{11}$$

The effect of using such a calculated flip angle series for different relaxation times is illustrated in Fig. 6, showing groups of curves representing the signal intensity as a function of the scan number. In each group, one fixed $T_{1,assumed}$ value is used for the cal-

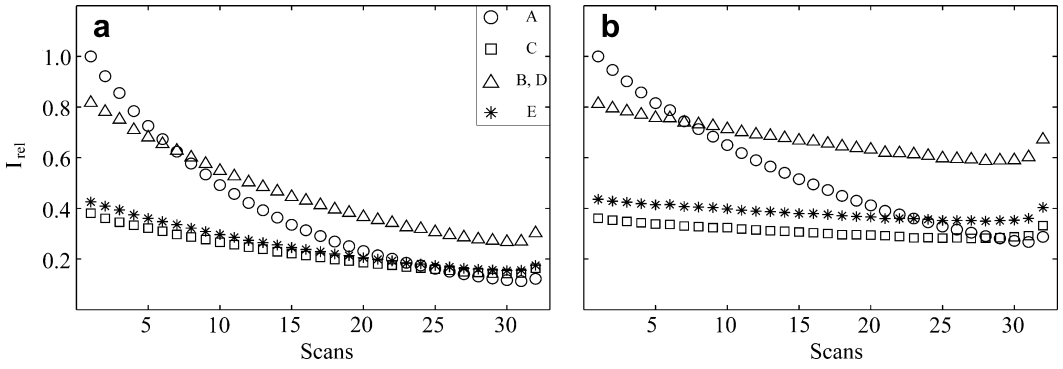

Fig. 5. Signal intensities of successive scans in variable flip angle experiments using hyperpolarized vanillin. The integrals of each of the four peaks are plotted vs. the number of scan. In (a), the flip angle series is calculated using Eq. (1); in (b), the flip angle series is calculated using Eq. (10). After dissolution, 32 small flip angle 1D ^{1}H spectra were acquired at an offset of 7 ppm, with an acquisition time of 138 ms for each spectrum. The total duration between adjacent small flip angle pulses was t = 200 ms, yielding a total NMR experiment time of 6.4 s. The relaxation time in formula 10 takes a value of 5 s. The letters in the legend correspond to the structure of vanillin in Fig. 2. In a and b, the largest respective intensity has been assigned a relative intensity I_{rel} = 1.

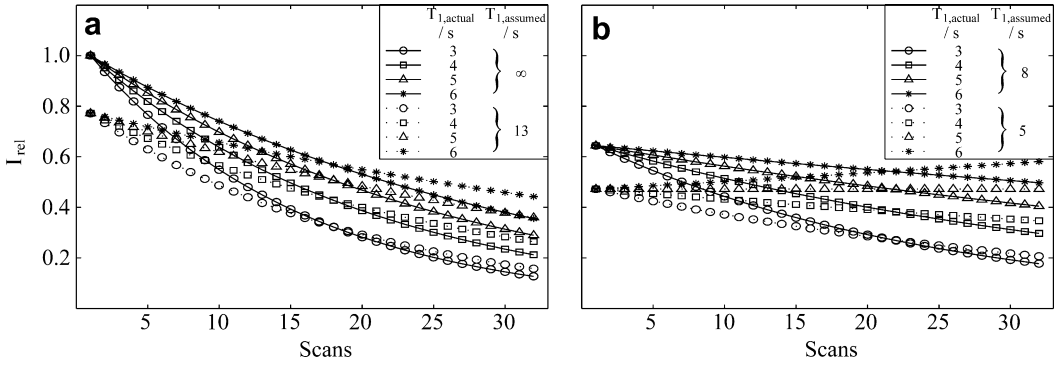

Fig. 6. Simulated intensities for successive scans in variable flip angle experiments. Each group of curves represents the intensities of signals from spins with actual T_1 = 3, 4, 5 and 6 s, calculated for the flip angle series (Eq. (10)) using one assumed value for T_1. In (a), assumed values for T_1 are ∞ and 13 s. In (b), assumed values are 8 and 5 s. The timing parameters used for the simulation are identical to the experimental parameters of Fig. 5. The scaling of I_{rel} is identical in both a and b.

culation of the flip angles, and the resulting signal is plotted for spins with different $T_{1,actual}$ values. If $T_{1,assumed}$ is larger than $T_{1,actual}$, the signal is reduced in later scans, whereas in the opposite case, the signal increases. On the other hand, the larger $T_{1,assumed}$, the larger the signal of the first scan. After Fourier transformation, a large $T_{1,assumed}$ value will therefore lead to a broad peak with large integral, whereas a small $T_{1,assumed}$ value will lead to a narrow peak with small integral. In the latter case, however, the time domain signal is substantially different from zero in the last scan, leading to a peak shape resembling a sinc function, also known as a truncation artifact. This effect then needs to be counteracted with apodization. In practice, in order to maximize the signal-to-noise ratio obtainable from a sample with given initial polarization, it may be advantageous to calculate the flip angle series using a $T_{1,assumed}$ value that is larger than the actual T_1 values of the molecule. Thereby, the reduction in signal intensity in later scans reinforces the apodization that would in any case be needed, and a larger initial signal can be obtained. Based on these considerations it appears that, while it may be beneficial to estimate T_1 relaxation times of the molecules under study for calculating optimal flip angles, the precise knowledge of those values is not required.

3.4. Polarization levels

The final concentration of vanillin was determined by HPLC to be 0.9–1.0 mM for the [^{13}C,^{1}H]-HMQC-experiment and 4.2 mM for the [^{1}H,^{13}C]-HMQC-experiment. To estimate the levels of polarization, single scan 1D ^{1}H and ^{13}C spectra were acquired with the same parameters as the first scan of the [^{13}C,^{1}H]-HMQC-experiment (with π pulse on ^{1}H) and the [^{1}H,^{13}C]-HMQC-experiment, respectively. The small flip angle pulse was replaced with a $\pi/2$ pulse, and a 4.1 M vanillin sample in DMSO-d6 was used as a standard for this purpose. In the dataset presented in Fig. 2 ([^{13}C,^{1}H]-HSQC), we estimate a polarization level between 2% and 4% by comparison with the thermally acquired spectrum of the first transient, using the equations published elsewhere [8]. In the [^{1}H,^{13}C]-HSQC spectrum in Fig. 4, the polarization level was between 2% and 7% for all resonances. These polarization levels are in agreement with values that we have reported previously using the same instrumentation [8].

3.5. Performance under non-stationary conditions

The major mechanism of signal loss in ex-situ DNP is relaxation during sample injection; the signal gain afforded by the DNP process is effectively lost if the time required for sample injection and stabilization is more than three to four times the spin-lattice relaxation time T_1. In contrast, a major advantage of DNP enhanced NMR is the ability to measure time-resolved NMR spectra of chemical processes that occur after admixing of a second reactant to a DNP polarized sample [13]. To obtain a mixing dead time that is comparable to the high time resolution achievable in these experiments, it is necessary to measure an NMR spectrum as rapidly as possible after mixing of two sample components. Using a sample injector described elsewhere [13], the spectra presented here were measured approximately 2.5 s after dissolution of the sample that has been polarized in the solid state, with a stabilization time of 200 ms. Rapid sample injection is however also concomitant with the need for measuring an NMR spectrum while residual fluid motion is still present in the NMR sample. Under these conditions, pulsed field gradients can lead to incomplete refocusing of coherences, and to attenuation of the observed signal. Indeed, a quantitative measurement of signal attenuation by pulsed field gradients is often used for the determination of diffusion coefficients by NMR [22]. The pulse sequence in Fig. 1 is optimized towards minimizing such undesired effects of pulsed field gradients, and the experiments presented appear to be quite robust when applied to non-stationary samples.

4. Conclusions

We have described a scheme that allows the acquisition of two-dimensional NMR spectra from a single DNP polarized sample. The present pulse sequence acquires the indirect spectral dimension sequentially, rather than distributed over space in the sample volume [4] or derived indirectly [8]. An advantage of this technique over indirectly derived chemical shift information lies in its capability of resolving overlapping chemical shifts through dispersion in a second dimension, albeit at the expense of spectral resolution. When compared to simultaneous sampling schemes, sequential acquisition as it is proposed here certainly requires a longer total experiment time (1–3 s). However, the present sequence is simpler to implement, and it is particularly robust with respect to experimental variations such as sample motion after rapid injection. For these reasons, sequential 2D spectroscopy of DNP polarized samples appears well suited for the routine structure determination of mass-limited samples of small molecules. In addition, it may also be useful for the NMR based investigation of non-equilibrium chemical processes in real-time.

Acknowledgment

SB acknowledges support from a Texas A&M University diversity fellowship, as well as from the Texas A&M Chemistry–Biology Interface (CBI) program. CH thanks the Camille and Henry Dreyfus Foundation for a New Faculty Award. Support from the Welch Foundation (Grant A-1658) and from Texas A&M University start-up funds is gratefully acknowledged.

References

[1] A. Abragam, M. Goldman, Principles of dynamic nuclear-polarization, Rep. Prog. Phys. 41 (1978) 395–467.
[2] J.H. Ardenkjaer-Larsen, B. Fridlund, A. Gram, G. Hansson, L. Hansson, M.H. Lerche, R. Servin, M. Thaning, K. Golman, Increase in signal-to-noise ratio of >10, 000 times in liquid-state NMR, Proc. Nat. Acad. Sci. USA 100 (2003) 10158–10163.
[3] S.E. Day, M.I. Kettunen, F.A. Gallagher, D.E. Hu, M. Lerche, J. Wolber, K. Golman, J.H. Ardenkjaer-Larsen, K.M. Brindle, Detecting tumor response to treatment using hyperpolarized ^{13}C magnetic resonance imaging and spectroscopy, Nat. Med. 13 (2007) 1382–1387.
[4] L. Frydman, D. Blazina, Ultrafast two-dimensional nuclear magnetic resonance spectroscopy of hyperpolarized solutions, Nat. Phys. 3 (2007) 415–419.
[5] M.E. Merritt, C. Harrison, C. Storey, F.M. Jeffrey, A.D. Sherry, C.R. Malloy, Hyperpolarized ^{13}C allows a direct measure of flux through a single enzyme-catalyzed step by NMR, Proc. Nat. Acad. Sci. USA 104 (2007) 19773–19777.
[6] C. Gabellieri, S. Reynolds, A. Lavie, G.S. Payne, M.O. Leach, T.R. Eykyn, Therapeutic target metabolism observed using hyperpolarized ^{15}N choline, J. Am. Chem. Soc. 130 (2008) 4598–4599.
[7] L. Frydman, T. Scherf, A. Lupulescu, The acquisition of multidimensional NMR spectra within a single scan, Proc. Nat. Acad. Sci. USA 99 (2002) 15858–15862.
[8] S. Bowen, H. Zeng, C. Hilty, Chemical shift correlations from hyperpolarized NMR by off-resonance decoupling, Anal. Chem. 80 (2008) 5794–5798.
[9] L. Zhao, R. Mulkern, C.H. Tseng, D. Williamson, S. Patz, R. Kraft, R.L. Walsworth, F.A. Jolesz, M.S. Albert, Gradient-echo imaging considerations for hyperpolarized ^{129}Xe MR, J. Magn. Reson. B 113 (1996) 179–183.
[10] M. Mishkovsky, L. Frydman, Progress in hyperpolarized ultrafast 2D NMR spectroscopy, Chem. Phys. Chem. 9 (2008) 2340–2348.
[11] A. Bax, R.H. Griffey, B.L. Hawkins, Correlation of proton and ^{15}N chemical-shifts by multiple quantum NMR, J. Magn. Reson. 55 (1983) 301–315.
[12] W. Willker, D. Leibfritz, R. Kerssebaum, W. Bermel, Gradient selection in inverse heteronuclear correlation spectroscopy, Magn. Reson. Chem. 31 (1993) 287–292.
[13] S. Bowen, C. Hilty, Time-resolved dynamic nuclear polarization enhanced NMR spectroscopy, Angew. Chem. Int. Ed. 47 (2008) 5235–5237.
[14] J. Keeler, D. Neuhaus, Comparison and evaluation of methods for two-dimensional NMR-spectra with absorption-mode lineshapes, J. Magn. Reson. 63 (1985) 454–472.
[15] G. Bodenhausen, H. Kogler, R.R. Ernst, Selection of coherence-transfer pathways in NMR pulse experiments, J. Magn. Reson. 58 (1984) 370–388.

[16] A.J. Shaka, P.B. Barker, R. Freeman, Computer-optimized decoupling scheme for wideband applications and low-level operation, J. Magn. Reson. 64 (1985) 547–552.
[17] A.J. Shaka, R. Freeman, Composite pulses with dual compensation, J. Magn. Reson. 55 (1983) 487–493.
[18] P.K. Mandal, A. Majumdar, A comprehensive discussion of HSQC and HMQC pulse sequences, Concepts Magn. Reson. A 20A (2004) 1–23.
[19] D. Moskau, Application of real time digital filters in NMR spectroscopy, Concepts Magn. Reson. 15 (2002) 164–176.
[20] J. Cavanagh, W.J. Fairbrother, A.G. Palmer, N.J. Skelton, Protein NMR spectroscopy: principles and practice, Academic Press Inc., San Diego, 1996.
[21] R.R. Ernst, G. Bodenhausen, A. Wokaun, Principles of nuclear magnetic resonance in one and two dimensions, Oxford University Press, New York, 1986. pp. 102, 333–335.
[22] E.O. Stejskal, Use of spin echoes in a pulsed magnetic-field gradient to study anisotropic restricted diffusion and flow, J. Chem. Phys. 43 (1965) 3597–3603.